Available online at www.sciencedirect.com

ScienceDirect

Procedia Materials Science 8 (2015) 986 – 993

Procedia Materials Science

www.elsevier.com/locate/procedia

International Congress of Science and Technology of Metallurgy and Materials, SAM - CONAMET 2013

Study of Plastic Heterogeneity in a Low Carbon Steel Sheet by EBSD

Javier Signorelli[a,b]*, Andrea Fourty[a,b], Analía Roatta[a,b], Claudio Schwindt[a,c], Fernando Schlosser[a,c], Raúl Bolmaro[a,b]

[a]*Instituto de Física Rosario (IFIR-CONICET), Bv. 27 de febrero 210 bis, (2000) Rosario, Argentina*
[b]*Facultad de Cs. Exactas, Ing. y Agrimensura (FCEIA-UNR), Av. Pellegrini 250, (2000) Rosario, Argentina*
[c]*Departamento de Metalurgia. UNS, Av. Alem 1253 (8000) Bahía Blanca, Buenos Aires*

Abstract

The aim of this study is to analyze the development of plastic heterogeneity in low carbon steel sheets when they are subjected to different loading paths, typical of forming process operations. Nakajima type tests are performed and employed to determine the Forming Limit Curve. This study attempts to characterize, at polycrystalline level, the plastic heterogeneity and its gradients, enabling the definition of correlations between the dislocation structure, grain size and crystallographic orientations. Geometrically Necessary Dislocations (GND) is estimated by calculating the curvature tensor from the measured orientation field. The results are compared with the Kernel Average Misorientation factor (KAM), normally available in the TSL- OIM EBSD software. The Quantification of the distribution of disorientations in each grain is performed by evaluating the second-order central moment of crystal misorientations (**Q** tensor). Finally, the evaluation of the isotropic and anisotropic factors of the **Q** tensor and the distribution of the misorientation preferential axes allow characterizing the microstructure dependent on the applied loading, the grain size or the crystal orientation.

Selection and peer-review under responsibility of the scientific committee of SAM - CONAMET 2013

* Corresponding author. Tel.: +54-0341-4808545; fax: +54-0341-4821772
E-mail address: signorelli@ifir-conicet.gov.ar

Selection and peer-review under responsibility of the scientific committee of SAM - CONAMET 2013
doi:10.1016/j.mspro.2015.04.160

Keywords: Dislocation structure heterogeneity, EBSD, GND

1. Introduction

Plastic deformation in polycrystalline metals is by its own nature an inhomogeneous process. During plastic deformation, the accumulation of dislocations produce high angle boundaries inside the grains, rendering differences in orientations inside them, and leading to subdivision of the grains into smaller domains with different orientations. The distribution of these structures is not random, they frequently show a predominant orientation as in the case of the rolling process, Liu et al. (1998). An always important aspect is the capacity to obtain a real measure of the observed microstructure, i.e. to be able to define the micro structural state of the material. Frequently, the dislocation structure is described in terms of two types of distributions: the statistically stored dislocations (SSD) and the geometrically necessary dislocations (GND). The last ones contribute to the curvature and fragmentation of the crystal lattice, Nye (1953) and Ashby (1970). Although it is known that the contribution of the GND is relatively small in the total density of dislocations, its effects may have a significant impact when certain strain states are applied to the material, Ma et al. (2006). In the present, because of the improved resolution of new microscopes (FEG-SEM) with high speed of data acquisition and indexing processing, EBSD (Electron Back Scatter Diffraction) systems allow to characterize, with an acceptable precision, the crystal orientation distribution and the spatial variation of the crystal orientations within domains of a few grains. As a consequence, knowing the orientations distributions (in 2D) makes it possible to estimate the density of GND as a result of evaluating 5 components of the Nye dislocations density tensor, which at the same time are defined by the curvature of the lattice that is compatible with the measured orientations field. High GND values are associated to grain boundaries or interfaces between phases with high contrast between its deformation values as it is the case of dual-phase steels, Hughes et al. (2003). To develop models capable of including these aspects of microstructure, they need to be extremely local approximations and include statistical aspects of the dislocations structure and yet this does not guarantee an adequate framework. In this sense, the present work is important for the development and validation of crystal plasticity models that pretend to include details of the microstructure developed in the material as a result of its plastic deformation. The combination of experimental tests and crystal plasticity models should be able to provide relevant information about the influence and relation of the resulting microstructure (GND) with the appearance of inadmissible stresses, which lead to the degradation of the material.

The aim of the present work is to characterize the microstructure induced by the deformation process by the analysis of the orientations field obtained with EBSD of specimens that were deformed by strain states that are typical in sheet forming processes. These may vary from uniaxial to biaxial tension, including also plane strain. These are the tests which are utilized in the determination of the forming limit diagram of rolled materials, Signorelli et al. (2012) and Serenelli et al. (2011). The study is intended to characterize at polycrystalline scale the heterogeneity in the plastic strain and its gradients, allowing finding a relation between the structure of dislocations, the grains size and the resulting crystals orientations. The quantification of the disorientations distribution inside each grain is carried out by evaluating the central second order moment of the crystal disorientation.

2. Material, test and characterization

The material used in the present work is an electro galvanized rolled steel sheet of DQ (drawing quality) type, with a thickness of 0.67 mm. The chemical composition is detailed in Table 1.

Table 1. Chemical composition of the steel sheet.

Element	C	P	S	Mn	Si	Cr	Ni	Cu	Mo	Al	N (ppm)
Wt %	0.070	0.020	0.009	0.300	0.040	0.020	0.010	0.010	0.010	0.192	88

The samples were subjected to the Nakajima test, typical for finding the forming limit curve of the material, varying the geometry of the samples in order to obtain different strain states with the same machine and die (Fig. 1). The details of the tests can be found in Signorelli et al. (2012).

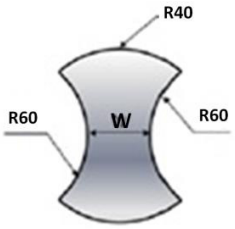

Nomen.	HG20	HG30	HG40	HG45	HG50	HG60	HG70	HG80
W(mm)	20	30	40	45	50	60	70	80

Fig. 1. Details of the samples used to obtain different strain states of the sheet

The circular samples, with adequate lubrication, are very close to balanced biaxial strain; the ones with intermediate central width (40, 45 and 50 mm) are very close to plane strain condition; while the thinner test pieces (20 and 30 mm) tend to uniaxial strain. The results shown in the present work correspond to the samples grayed in Fig. 1.

The microstructure and crystallographic texture of the material were obtained, both in its initial and deformed state, with a FEG-EBSD equipment. In our case, as the mechanical tests were conducted until necking, it was very important how we chose the region of the sample to be analyzed. For each of the samples, an area, still homogeneous but very close to the necking zone, is selected in order to analyze a state close to the one that produced failure. The samples extracted in this way are approximately 3-5 mm long each side. The type of scanning was selected depending on what kind of information was needed: i) with a broad scanning over approximately 200 µm x 200 µm with a 2 µm step we obtained the grain sizes and distribution, and the crystallographic texture and ii) with a finer scanning over an area of approximately 90 µm x 90 µm with a step of 0.1 µm we obtained the microstructural characterization. Fig. 2 shows the EBSD map that was obtained for the material in its initial state. The high percentage of grains colored with blue and violet reveal a high amount of orientations located at the gamma fiber (<hkl>{111}). Although the sample has been extracted from the undeformed sheet, the orientations map reveals the existence of a remnant substructure originated by the previous rolling process.

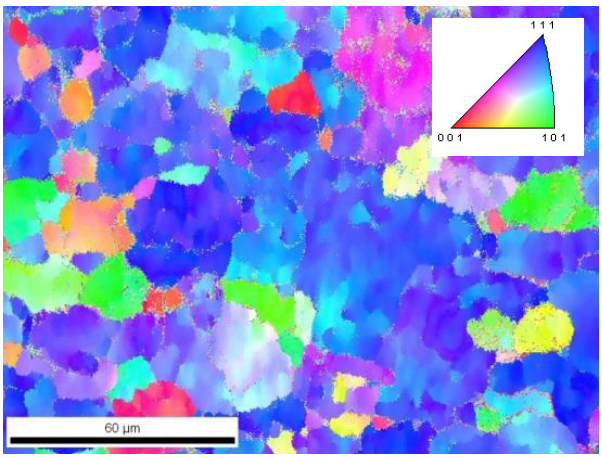

Fig. 2. EBSD map of initial state of the material. Inverse pole figures. Scanning of 200 µm x 200 µm with a 2 µm step.

The ability to characterize the crystallographic texture with EBSD is in our case, a critical issue, because the tested samples, due to their hemispherical shape, can only be inspected in very small regions of about 2.5 x 2.5 mm^2. These sizes do not satisfy the minimum area required for a satisfactory texture determination, as can be obtained with X-ray diffraction techniques, due to the characteristic strain inhomogeneity. Table 2 is a summary in terms of ideal orientation components (misorientation of less than 15 degrees) of the results obtained in unstrained samples in which both measuring techniques were applied.

Table 2. Volume fraction of ideal components calculated as crystal orientations obtained by X-ray and EBSD techniques.

	<110>{001}	<110>{112}	<110>{111}	<121>{111}	<225>{554}	Others
X-ray [%]	1.4	5.5	11.6	7.3	9.2	60.0
EBSD [%]	0.8	0.6	20.5	12.0	10.4	55.7

Even though differences are observed when comparing components, the global aspect of the texture obtained by EBSD keeps the main characteristics observed when utilizing X-rays. EBSD maps are processed by an algorithm that groups sets of connected and similarly oriented points into “grains”. The neighbors of each point are checked to see if they are within the grain tolerance angle (2 degree in our case). If a neighboring point is found to be within the tolerance angle then the neighbors of this point are checked to see if they are within the tolerance angle of this point. The procedure is repeated over and over until the set of connected grains is bounded by points, that exceed the tolerance angle to their neighbors (TSL-OIM manual). Using last procedure we found approximately 4000 grains, which is in the range of the 2000–10000 suggested by Wright and Kocks (1996) and Hutchinson et al. (1999) for statistically significant “bulk” texture. In the present case it is observed that 4000 orientations are still insufficient to simultaneously have qualitative and quantitative descriptions.

3. Results and discussion

It is usual when working with crystallographic texture to describe the orientations in terms of the Euler angles. This representation, although very simple to understand, has the problem that it is not in an Euclidean space, making the calculations very cumbersome to perform. In order to work in an Euclidean space, we utilize axis-angle and quaternion representations. The orientation of the lattice, given as a rotation unitary axis $\hat{r}$ and an angle ω with respect to a reference system, can be combined in a quaternion; among many other attractive properties, they offer the most efficient known way for performing computations on combining rotations, which has some advantages for the calculations we propose. So, a quaternion is defined as:

$$\mathbf{q} = (q_0; \hat{q}) = (\cos(\tfrac{\omega}{2}); \hat{r}\sin(\tfrac{\omega}{2})) \tag{1}$$

The difference in orientation between A and B is given by $\Delta\mathbf{q} = \mathbf{q}_A^{-1}\mathbf{q}_B$ As this is the difference in orientation between two points of a crystal lattice it is necessary to include in the analysis the symmetries of the lattice. Being all the equivalent descriptions of a given misorientation represented by S, it results that:

$$\Delta\mathbf{q}_S = \mathbf{q}_A^{-1}S_A^{-1}S_B\mathbf{q}_B = \mathbf{q}_A^{-1}S\mathbf{q}_B \tag{2}$$

Between all the equivalent misorientations it is selected the one that corresponds to the minimum angle $\theta = 2\min\{\arccos(\Delta q_{0s})\}$. This disorientation, which will be useful to calculate the dislocation density, contains information about the angle and the rotation axis.

3.1. Dislocation density tensor

Since the accumulation of dislocations in the crystal lattice is associated to its curvature, it is deduced that the dislocation density tensor $\boldsymbol{\alpha}$ is directly related with the lattice curvature tensor $\mathbf{k}$, by $\boldsymbol{\alpha} = \mathbf{k}^T - \mathrm{tr}(\mathbf{k})$, He et al. (2008). Knowing the disorientation between two proximate points, the rotation of the lattice can be expressed by:

$$\Delta\hat{\omega} = \theta\,\hat{r} = \frac{2\arccos\Delta q_0}{\sqrt{1-\Delta q_0^2}}\Delta\hat{q} \approx 2\delta\hat{q} \quad \text{for } \theta << 1 \tag{3}$$

which permits us to approximate the curvature tensor in terms of the spatial change in the disorientation vector $\Delta\mathbf{q}$, as:

$$k_{kl} = \frac{\partial\omega_k}{\partial x_l} \approx 2\frac{\Delta\hat{q}_k}{\Delta x_l} \quad \text{for } k,l=1,2,3 \tag{4}$$

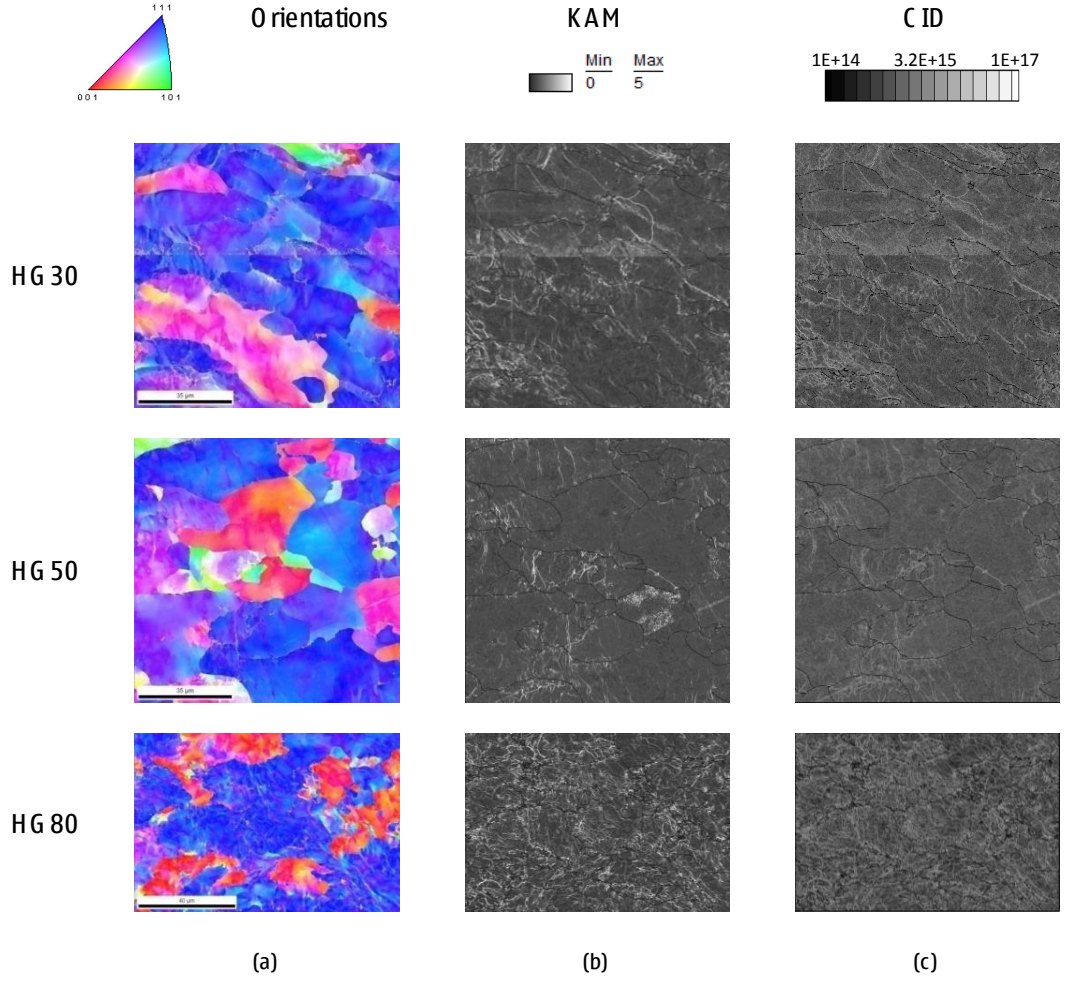

Fig. 3. Maps of the deformed material specimens in uniaxial tension (HG30), plane strain (HG50) and balanced biaxial strain (HG80). a) Inverse pole figures, b) KAM considering only the first neighbor and c) CID values. In all cases the scanning step was 0.1 μm.

where Δx_l represents the distance in the ¨l¨ direction between two pixels that are disoriented by $\Delta\mathbf{q}$. It is clear from the previous formula that, since the EBSD maps provide partial information of the orientation field, it is only possible to estimate 6 of the 9 components of the curvature tensor, and with these, only 5 components of the dislocation density tensor:

$$\alpha_{12}=k_{21};\quad \alpha_{13}=k_{31};\quad \alpha_{21}=k_{12};\quad \alpha_{23}=k_{32};\quad \alpha_{33}=-k_{11}-k_{22} \tag{5}$$

Finally, we introduce an approximate measure or apparent dislocations density ρ^* to characterize the total density of GND, which is called Curvature Induced Dislocation (CID) density.

$$\rho^* = \frac{1}{b}\|\boldsymbol{\alpha}\|_\infty = \frac{1}{b}\left(|\alpha_{12}|+|\alpha_{13}|+|\alpha_{21}|+|\alpha_{23}|+|\alpha_{33}|\right) \tag{6}$$

where b represents the Burgers vector module of the material. Although it is possible to generalize the previous equation for the case of materials where the active deformation systems have different Burgers vectors, the analysis is restricted for simplicity to cubic materials with a unique value of the referred vector. When adjacent pixels belong to different grains an arbitrary $\rho^* = 0$ value is assigned.

Fig. 3 shows the structure of CID that was found in the samples extracted from the tested specimens in uniaxial tension (HG30), plane strain (HG50) and balanced biaxial strain (HG80), which were tested until the limit strain. In all cases a fine scanning of 0.1 μm step was carried out. For comparative purposes the KAM (Kernel Average Misorientation) values are also included. The KAM parameter gives, for every pixel j of the sample, the mean value of the difference in orientation θ_{jk} with the neighboring pixels k:

$$\mathrm{KAM(j)} = \frac{1}{k}\sum_k \theta_{jk} \tag{7}$$

The KAM values are usually available in the commercial software, and, although it is a valid representation of the measured disorientations field, it restricts the information to the disorientation angle and does not include the rotation axis, contrarily to the CID value which involves the whole quaternion. Nevertheless, a good visual correlation between both measurements, in most of the grains, has been obtained. Using similar criteria grain boundaries are seen as black lines in KAM maps.

3.2. Orientation distribution inside grains

An aspect that is always difficult to clarify is whether it is possible, from the KAM and/or CID maps, to get information about the accumulation of GND as a function of the crystal orientation of the grain or another of its characteristics. As the dislocations density distribution inside the grain is inherently an inhomogeneous property, the mean value of a grain is not always representative of the real structure. However, visual differences in the KAM and CID fields can be observed for the HG30 and HG50 specimens with respect to the HG80 (Fig. 3). These differences are not related to the maximum values of GND, but to the structure of the lines of high density of GND. A possible way to capture at least part of this phenomenon is evaluating the second order central moment tensor of the distribution, **Q**, which permits to express with scalar values the orientations distribution inside a selected region. To obtain this tensor the mean orientation of a group of orientations is calculated as:

$$\bar{\mathbf{q}} = \frac{1}{N}\sum_{i=1}^{m}\mathbf{q}_i \quad \text{, being } N = \left\|\sum_{i=1}^{m}\mathbf{q}_i\right\| \tag{8}$$

The difference in orientations between each individual orientation and the mean one is defined as $\delta\mathbf{q}_i = \mathbf{q}_i\bar{\mathbf{q}}^{-1}$ requiring the condition that the symmetrically equivalent orientation closest to the mean one is always selected. Using this difference in orientation for each orientation of a set (e.g. pixels that belong to the same grain) the tensor **Q** can be calculated:

$$\mathbf{Q} = \frac{1}{m}\sum_{i=1}^{m}\delta\hat{q}_i \otimes \delta\hat{q}_i \tag{9}$$

An interesting attribute of this characterization is that the tensor **Q** is independent of the value of the mean orientation, $\bar{\mathbf{q}}$, since the mean value of the disorientation vector is zero. This tensor provides three parameters: the distribution width, its anisotropy and a preferential rotation axis defined by its eigenvalues and eigenvectors. Its three eigenvalues, λ_i, which are not negative (**Q** is semi-defined as positive), provide information about the standard deviation in the three principal directions, $\sigma_i = \sqrt{\lambda_i}$ and the mean geometric value of them, $\bar{\sigma} = \sqrt[3]{\sigma_1\sigma_2\sigma_3}$, describes the isotropic spread (distribution width). The ratio of the highest of the standard deviations to the mean geometric value defines the anisotropy of spread, which characterizes the anisotropy of the orientations distributions. The preferential rotation axis is given by the eigenvector that corresponds to the highest of its eigenvalues, He et al. (2008).

Fig. 4a shows the isotropic and anisotropic spread of the four analyzed test samples as a function of the grain size of the material. The initial state of the material presents, as expected, the lowest isotropic dispersion while the highest one is for the case of balanced biaxial strain. This is in concordance with the fact that the network of high values of GND is more pronounced in the HG80 specimen (Fig. 3c). In the case of anisotropy of spread the results are very similar for all the analyzed cases showing a rise in the values when the grain size decreases. It is also interesting to examine these parameters related to the typical directions on the sheet, as shown in Fig. 4b. It is observed that both, the initial specimen and the one deformed in plane strain, present the lowest isotropic dispersion values, being this fact mainly visible in the γ fiber, where the specimens subjected to uniaxial and balanced biaxial strain show a clear difference.

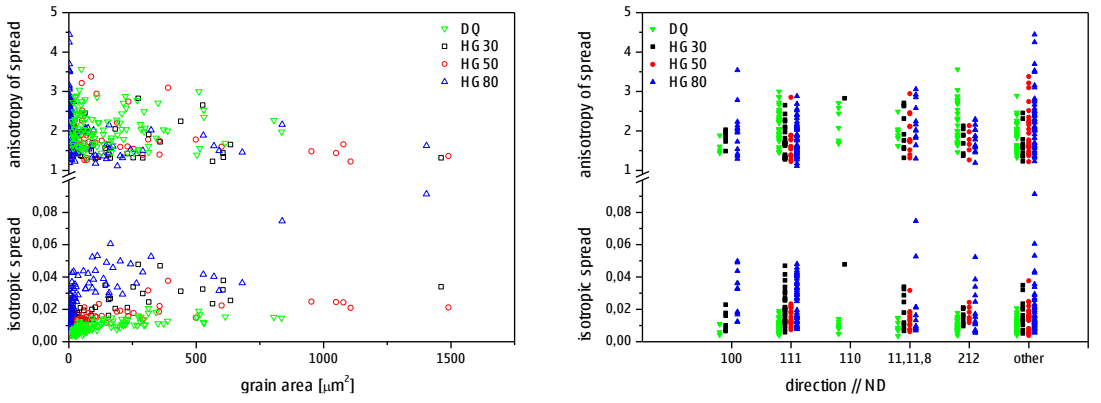

Fig.4. Isotropic and anisotropy of spread in the initial state and in different strain states as a function of: a) grain size b) crystal direction parallel to the sheet normal

The eigenvector corresponding to the maximum eigenvalue characterizes the dominant rotation axis of the group of disorientations inside the grains. Fig. 5 shows the projections, as pole figures, of the locations of the preferential

rotation axes in the analyzed test pieces, with respect to a reference system attached to the sheet. The distribution of these rotation axes exhibit a clear evolution from its initial state. It is as well observed a large randomness for the case of balanced biaxial strain, as it is expected due to the symmetry of the test.

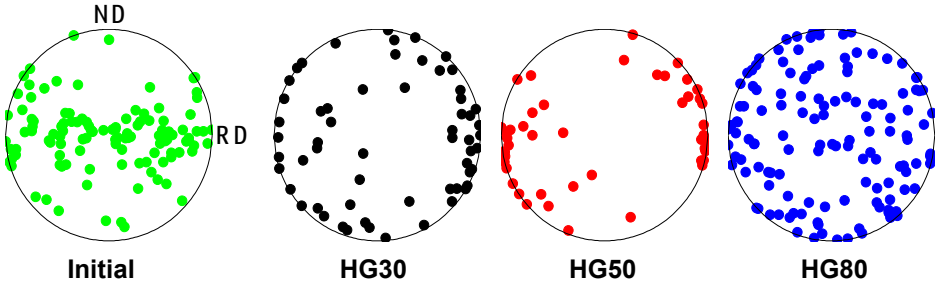

Fig. 5. Preferential rotation axis as a function of the strain state. The axis of each grain is referred to a reference system attached to the sheet.

4. Conclusions

The CID dislocations structure in electro-galvanized steel sheets of drawing quality type was characterized in its initial state and deformed in different strain states, as uniaxial tension, plane strain and balanced biaxial strain until deformations that were close to the previously known limit strains. The GND density was estimated using an estimation of the Nye tensor based in the evaluation of the lattice curvature tensor obtained from the orientation map measured by EBSD. A good visual correlation in most of the grains between KAM and CID distributions is observed. The calculation of the CID contains a higher level of information than the one of the KAM, because it includes not only the angle of disorientation but also the rotation axis and permits to conduct a deeper analysis of the EBSD orientation maps.

Finally, while from this work we cannot firmly conclude about the expected correlations, the adequate processing of the information contained in the EBSD maps permits to obtain relevant information to characterize the microstructure of an important number of crystals. In this sense it was observed that the isotropy and anisotropy of the spread of grain orientations and the distribution of preferential disorientation axes are suitable parameters to observe differences that depend on the type of applied external load, grain size or crystal orientation.

References

Ashby, M.F., 1970. The deformation of plastically non-homogeneous materials, Philosophical Magazine, 21, 399-424.

He, W., Ma, W., Pantleon, W., 2008. Microstructure of individual grains in cold-rolled aluminium from orientation inhomogeneities resolved by electron backscattering diffraction, Materials Science & Engineering, A 494, 21-27.

Hughes, D.A, Hansen, N., Bammann, D.J., 2003. Geometrically necessary boundaries, incidental dislocation boundaries and geometrically necessary dislocations, Scripta Materialia, 48,147-153.

Hutchinson, W.B., Lindh, E. and Bate, P.S., 1999. Proc. 12th Int. Conf. on Texture, ed. J. Szpunar, NRC Press, Ottowa, 34.

Liu, Q., Jull Jensen, D., Hansen, N., 1998. Effect of grain orientation on deformation structure in cold-rolled polycrystalline aluminium, Acta Materalia. 46, 5819-5838.

Ma, A., Roters, F., Raabe, D., 2006. A dislocation density based constitutive model for crystal plasticity FEM including geometrically necessary dislocations, Acta Materialia, 54,2169-79.

Nye, J.F., 1953. Some geometrical relations in dislocated crystals, Acta Metallurgica, 1, 153-162.

Signorelli, J.W., Serenelli, M.J., Bertinetti, M.A., 2012. Experimental and numerical study of the role of crystallographic texture on the formability of an electro-galvanized steel sheet, Journal of Materials Processing Technology, 212, 1367-1376.

Serenelli, M.J., Bertinetti, M.A., Signorelli, J.W., 2011. Study of limit strains for FCC and BCC sheet metal using polycrystal plasticity, International Journal of Solids and Structures 48, 1109–1119.

Wright, S.I. and Kocks, U.F, 1996. Proc. 11th Int. Conf. on Texture. Xian, ed. Z. Liang, Int. Academic Publishers, Beijing, 1, 53.